Relationship between lamina cribrosa curvature and the microvasculature in treatment-naïve eyes

Ji-Ah Kim,[1] Tae-Woo Kim,[1] Eun Ji Lee,[1] Michael J A Girard,[2,3] Jean Martial Mari[4]

ABSTRACT

Background/Aims To investigate the relationship between the lamina cribrosa (LC) curvature and the microvasculature within the LC in treatment-naïve eyes with normal-tension glaucoma (NTG) and in healthy eyes.

Methods Forty-one eyes with treatment-naïve NTG and 41 age and sex-matched healthy control eyes were included. The optic nerve head (ONH) area was scanned using spectral-domain optical coherence tomography (OCT) to examine the LC curvature quantified as the LC curvature index (LCCI). OCT angiography of the ONH area was performed to determine the LC vessel density (LCVD) in the en face images obtained from the layer segmented at the level of the LC. The LCVD was calculated as the percentage area occupied by vessels within the measured region.

Results The LCCI was larger (9.53 ± 1.33 vs 6.55 ± 1.02, p<0.001) and LCVD was smaller ($28.0\% \pm 6.1\%$ vs $35.2\% \pm 6.3\%$, p<0.001) in NTG eyes than in healthy eyes. There were overall significant associations of a smaller retinal nerve fibre layer (RNFL) thickness (p<0.001), a smaller visual field mean deviation (MD) (p=0.003) and a larger LCCI (p≤0.004) with a smaller LCVD. In NTG group, the LCVD was positively associated with the RNFL thickness (p=0.012) and visual field MD (p=0.023), and negatively associated with the axial length (p≤0.013) and LCCI (p≤0.007). In healthy group, a smaller RNFL thickness (p=0.023) was associated with a smaller LCVD.

Conclusion A larger LCCI was significantly associated with a smaller LCVD in treatment-naïve NTG eyes but not in healthy eyes, indicating that mechanical strain potentially influences the perfusion within the LC in eyes with NTG.

INTRODUCTION

Glaucoma is a multifactorial disease, with mechanical stress and decreased perfusion in the optic nerve head (ONH) being considered two principal mechanisms of glaucomatous axonal damage. Deformation of the lamina cribrosa (LC) has been proposed as a key phenomenon underlying the pathogenesis of glaucoma.[1–4] The LC deformation may impose mechanical stress on the axons that pass through the laminar pores, leading to a blockade of axoplasmic transport that may finally result in the apoptosis of retinal ganglion cells (RGC).[5 6] Deformation of the capillary containing laminar beams may also decrease perfusion to the laminar segments of the axons that leads to ischaemic damage of the RGCs.[7]

The curvature of the LC has been recently proposed as a reliable parameter for quantifying LC deformation.[8 9] The LC curvature was found to be significantly associated with glaucoma development[10] and progression,[11] suggesting that the LC curvature is a good indicator of the mechanical stress exerted on the LC. On the other hand, the LC curvature decreases following trabeculectomy, which may indicate that decreasing the intraocular pressure (IOP) reduces the imposed mechanical stress.[12] We recently found that the decrease in the LC curvature after trabeculectomy accompanies an increase in the microvasculature at the level of the LC.[13] Based on this result, it could be speculated that decreased mechanical strain indicated by the reduction in the LC curvature also reduces the compression of the laminar capillaries.

It is possible that IOP-lowering treatment reduces mechanical strain, and at the same time enhances perfusion of the ONH. If that is the case, the microvasculature of the LC could serve as a potential marker representing ONH perfusion associated with the mechanical strain. The purpose of the present study was to determine whether the mechanical strain within the LC was associated with the LC microvasculature. This study therefore investigated the relationship between the LC curvature and the LC microvasculature in treatment-naïve eyes with normal-tension glaucoma (NTG) and in healthy eyes.

MATERIALS AND METHODS

This study involved subjects with NTG and healthy participants who were enrolled in ongoing prospective study (Investigating Glaucoma Progression Study) at the Glaucoma Clinic of Seoul National University Bundang Hospital. Informed consent was obtained from all subjects.

Study subjects

Comprehensive ophthalmic examinations included assessments of best corrected visual acuity, a refraction test, slit-lamp biomicroscopy, Goldmann applanation tonometry, gonioscopy, stereo disc photography and red-free fundus photography (Kowa VX-10; Kowa Medicals, Torrance, CA, USA). Other ophthalmic examinations included scanning of the circumpapillary retinal nerve fibre layer (RNFL) and the ONH using spectral-domain optical coherence tomography (OCT; Spectralis, Heidelberg Engineering, Heidelberg, Germany), swept-source OCT angiography (OCTA; DRI OCT Triton, Topcon, Tokyo, Japan) and standard automated perimetry (Humphrey Field Analyzer II 750, 24-2 Swedish interactive threshold algorithm, Carl Zeiss Meditec, Dublin, CA, USA). Subjects also underwent measurements of central corneal

thickness (Orbscan II, Bausch & Lomb Surgical, Rochester, NY, USA), corneal curvature (KR-1800, Topcon) and axial length (IOLMaster V.5, Carl Zeiss Meditec).

The medical history was also taken from subjects, including the presence of cold extremities, migraine, family history of glaucoma and other systemic conditions. Digital automatic blood pressure (BP) monitor (Omron HEM-770A, Omron Matsusaka, Matsusaka, Japan) was used to measure the systolic and diastolic BPs. The mean arterial pressure (MAP) was calculated as diastolic BP+1/3(systolic BP–diastolic BP), and the mean ocular perfusion pressure was calculated as 2/3(MAP–IOP) at the time of OCTA.

Eyes included in the NTG group were required to have a record of untreated IOP. Healthy subjects were 1:1 matched with the patients with NTG in terms of age and sex. Definition of NTG and healthy eye, and criteria for inclusion and exclusion are described in the online Supplementary appendix.

Measurement of LC curvature index
The LC curvature was evaluated at seven locations equidistant to the vertical optic disc diameter using horizontal B-scan images as described previously.[8 12] These seven B-scan lines, from the superior to the inferior regions, were defined as planes 1–7, respectively (online supplementary figure 1). In this model, plane 4 corresponds to the mid-horizontal plane, and planes 2 and 6 correspond approximately to the superior and inferior mid-periphery, respectively.

The LC curvature was determined using the LC curvature index (LCCI), which was determined by assessing the inflection of a curve representing a section of the LC.[8 12] A new reference line (LC surface reference line) was drawn on analysed B-scan by connecting the 2 points on the anterior LC surface that met the lines drawn from each Bruch's membrane (BM) termination point perpendicular to the BM opening reference line to measure the LCCI. The length of this reference line was defined as width (W), and the LC curve depth as the maximum depth from this reference line to the anterior LC surface (online supplementary figure 1). The LCCI was calculated as (LC curve depth/W)×100. Because the curvature was normalised to the LC width, it describes the shape of the LC independent of the actual size of the ONH. Because the LC was often not clearly visible outside this opening, only the LC within the BM opening was considered. In eyes with LC defects, the LCCI was measured using a presumed anterior LC surface that best fit the curvature of the remaining part of the LC or excluding the area of LC defect.

Before the measurement, the peripheral LC was postprocessed by using adaptive compensation to enhance its visibility.[14 15] Manual calliper tool in the Amira software (V.5.2.2, Visage Imaging, Berlin, Germany) was used to measure. The values measured from the seven B-scans were used to calculate the mean LCCI of the eye.

The LCCIs were measured by two experienced observers (JAK and EJL) who were masked to the clinical information. The average of the measurements from each of the two observers was used for analysis.

Measurement of LC vessel density
The microvasculature of the LC was evaluated in the en face OCTA images obtained from the segmented layer of the LC. The optic nerve and peripapillary area were imaged using a swept-source OCTA device (DRI OCT Triton, Topcon), as described previously.[13] B-scan image had an image quality score of ≥30. The eye was excluded when the artefacts blocked the vascular signal (eg, due to blinking or masking)[16] or when the quality of the OCTA images was poor (eg, due to blurring).

The DRI OCT Triton device shows the microvasculature in the layer of interest in a customised manner. En face OCTA images were produced in the segmented layer of the LC (from the anterior to posterior borders of the LC) as described previously using manual segmentation (online supplementary figure 2).[13] The scanned images were extracted from the OCTA instrument and imported into the publicly available ImageJ software (National Institutes of Health, Bethesda, Maryland, USA; http://imagej.nih.gov/ij/). The extracted en face images were binarised using Otsu's method because contrast among en face images can be different.[17] Otsu's method assumes that the image contains two classes of pixels following a bimodal distribution. It calculates optimum threshold by minimising intraclass variance and maximising interclass variance.[18] The black region was considered as vascular area and its number of pixels was quantified with ImageJ software. Region of interest (ROI) was determined based on the cup of disc where the LC vasculature is clearly visible in OCTA en face image (online supplementary figure 2). The area covered by large retinal vessels visible on colour disc photography or projection artefact was manually excluded from the ROI since DRI OCT Triton device does not provide projection-artefacts removal algorithm. The microvessel density in each ROI was defined as the LC vessel density (LCVD), which was calculated by dividing the number of pixels in the microvascular area by that of the ROI and expressed by percentage.

The LCVD was measured in a masked fashion by two experienced observers (JAK and EJL). The average of the measurements from the two observers was used for analysis.

Data analysis
The interobserver agreements for measuring the LCCI and LCVD were assessed by calculation of intraclass correlation coefficients (ICC) and 95% CIs. Comparisons between groups were performed using t-test for continuous variables and the χ^2 test for categorical variables. Regression analysis was used to investigate the factors associated with the LCVD. Only variables with p<0.10 in the univariate analysis were included in the multivariate model. All analyses were performed using SPSS (V.22.0, SPSS). P values <0.05 were considered to indicate statistical significance.

RESULTS
Ninety-three NTG eyes and 66 healthy eyes were initially included. Among them, 28 (18 NTG and 10 healthy eyes) were excluded due to the presence of a tilted or torted disc, and 31 (18 NTG and 13 healthy eyes) were excluded due to poor visualisation of the LC microvasculature due to either small ROI or poor image quality. After matching for age and sex, each group consisted of 41 eyes (a total of 82 eyes). Measurements of the LCCI and LCVD exhibited excellent interobserver agreement (ICC=0.980 and 0.977, respectively; 95% CI 0.969 to 0.987 and 0.964 to 0.985, respectively).

The online supplementary table compares the clinical characteristics of NTG and healthy subjects. Compared with the healthy group, the NTG group had a smaller global RNFL thickness, a smaller visual field mean deviation (MD), a larger mean LCCI and a smaller LCVD (all p<0.001).

Factors associated with LCVD were determined using linear regression analysis. Multivariate analyses were performed in two ways to avoid multicollinearity between the RNFL thickness and visual field MD. In both univariate and multivariate analyses, a

Table 1 Factors associated with the vessel density in the lamina cribrosa

Variables	Univariate		Multivariate 1*		Multivariate 2*	
	β (95% CI)	P value	β (95% CI)	P value	β (95% CI)	P value
Age, *per 1 year older*	−0.051 (−0.167 to 0.065)	0.383				
Male gender	0.315 (−2.840 to 3.470)	0.843				
Central corneal thickness, *per 1 µm larger*	0.014 (−0.030 to 0.058)	0.523				
Axial length, *per 1 mm larger*	−0.315 (−1.574 to 0.944)	0.620				
Baseline IOP, *per 1 mm Hg higher*	−0.416 (−1.088 to 0.256)	0.222				
Global RNFL thickness, *per 1 µm larger*	0.323 (0.239 to 0.407)	<0.001	0.221 (0.115 to 0.327)	<0.001		
Mean deviation, *per 1 dB larger*	0.942 (0.613 to 1.270)	<0.001			0.532 (0.185 to 0.879)	**0.003**
Mean LCCI, *per 1 unit larger*	−2.256 (−2.916 to −1.595)	<0.001	−1.176 (−1.970 to −0.382)	**0.004**	−1.661 (−2.400 to −0.922)	<0.001
Systolic BP, *per 1 mm Hg higher*	0.006 (−0.109 to 0.121)	0.917				
Diastolic BP, *per 1 mm Hg higher*	0.050 (−0.127 to 0.226)	0.576				
Mean arterial pressure, *per 1 mm Hg higher*	0.032 (−0.131 to 0.196)	0.693				
Mean ocular perfusion pressure, *per 1 mm Hg higher*	0.077 (−0.163 to 0.316)	0.525				
Self-reported hypertension	−0.294 (−3.845 to 3.258)	0.870				
Self-reported diabetes	1.592 (−3.699 to 6.884)	0.826				
Family history of glaucoma	0.778 (−5.263 to 6.818)	0.798				
Cold extremities	0.900 (−3.905 to 5.705)	0.710				
Migraine	−1.005 (−6.304 to 4.294)	0.707				

Values with statistical significance are in boldface.

*Only variables with p<0.1 in univariate analysis were included in the multivariate model.

BP, blood pressure; IOP, intraocular pressure; LCCI, lamina cribrosa curvature index; RNFL, retinal nerve fibre layer.

smaller global RNFL thickness (both p<0.001), a smaller visual field MD (p<0.001 and p=0.003, respectively) and a larger mean LCCI (p<0.001 and p≤0.004, respectively) were significantly associated with a smaller LCVD (table 1, figure 1).

The same analysis was performed separately in the NTG and healthy groups. In the NTG group, a smaller global RNFL thickness (p<0.001), a smaller visual field MD (p=0.001) and a larger mean LCCI (p=0.002) were significantly associated with a smaller LCVD (table 2). Multivariate analyses, which were performed in two ways to avoid multicollinearity between the RNFL thickness and visual field MD, revealed that a longer axial length (p≤0.013), a smaller global RNFL thickness (p=0.012), a smaller visual field MD (p=0.023) and a larger mean LCCI (p≤0.007) were significant factors associated with a smaller LCVD. In healthy eyes, both univariate and multivariate analyses revealed that a smaller global RNFL thickness (p=0.013 and p=0.023, respectively) was associated with a smaller LCVD (table 3).

Figure 2 illustrates two treatment-naïve NTG eyes in which a larger and a smaller LCCI were associated with a smaller and a larger LCVD, respectively.

DISCUSSION

The present study found a significant negative correlation between the LCCI and LCVD in treatment-naïve NTG eyes. There was no significant correlation in healthy control eyes. To our knowledge, this is the first study investigating the relationship between the LCCI and LCVD in both treatment-naïve glaucomatous and healthy human eyes.

Decreased perfusion in the ONH has been found in glaucomatous eyes using fluorescein angiography,[19] scanning laser Doppler flowmetry[20] and laser speckle flowgraphy.[20 21] Based on these findings, it has been suggested that decreased ONH perfusion is an independent pathogenic factor in glaucoma in addition to increased mechanical stress. However, from a biomechanical perspective, mechanical stress and perfusion impairment are interconnected.[7]

It is proposed that an increased mechanical stress in the LC can lead to decreased perfusion in the ONH axons via compression of the capillaries in the laminar beam. Given that the LCCI reflects mechanical strain of the ONH,[9 12] our finding of a smaller LCVD being associated with a larger LCCI supports
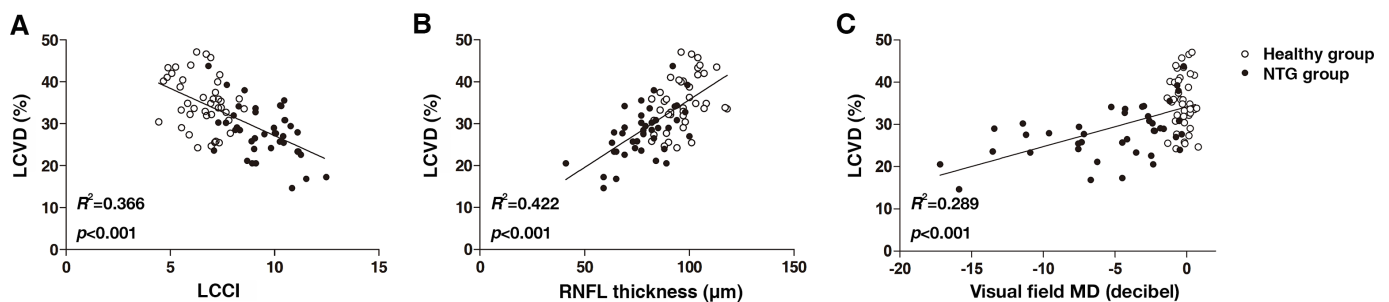
Figure 1 Scatterplots showing the correlation between the lamina cribrosa vessel density (LCVD) and lamina cribrosa curvature index (LCCI) (A), that between the LCVD and retinal nerve fibre layer (RNFL) thickness (B), and that between the LCVD and visual field mean deviation (MD) (C) in the healthy and normal-tension glaucoma (NTG) groups.

Table 2 Factors associated with the vessel density in the lamina cribrosa in treatment-naïve normal tension glaucomatous eyes

Variables	Univariate		Multivariate 1*		Multivariate 2*	
	β (95% CI)	P value	β (95% CI)	P value	β (95% CI)	P value
Age, *per 1 year older*	−0.034 (−0.181 to 0.112)	0.638				
Male gender	−2.318 (−6.133 to 1.497)	0.226				
Central corneal thickness, *per 1 µm larger*	0.014 (−0.037 to 0.065)	0.582				
Axial length, *per 1 mm larger*	−1.397 (−2.921 to 0.127)	0.071	−1.634 (−2.901 to −0.368)	**0.013**	−1.680 (−2.964 to −0.397)	**0.012**
Baseline IOP, *per 1 mm Hg higher*	−0.351 (−1.147 to 0.445)	0.377				
Global RNFL thickness, *per 1 µm larger*	0.281 (0.154 to 0.409)	**<0.001**	0.166 (0.038 to 0.294)	**0.012**		
Mean deviation, *per 1 dB larger*	0.652 (0.273 to 1.031)	**0.001**			0.410 (0.060 to 0.760)	**0.023**
Mean LCCI, *per 1 unit larger*	−2.139 (−3.442 to −0.837)	**0.002**	−1.707 (−2.915 to −0.500)	**0.007**	−2.224 (−3.342 to −1.105)	**<0.001**
Systolic BP, *per 1 mm Hg higher*	0.008 (−0.161 to 0.117)	0.921				
Diastolic BP, *per 1 mm Hg higher*	0.048 (−0.220 to 0.316)	0.717				
Mean arterial pressure, *per 1 mm Hg higher*	0.035 (−0.220 to 0.290)	0.780				
Mean ocular perfusion pressure, *per 1 mm Hg higher*	0.090 (−0.286 to 0.466)	0.628				
Self-reported hypertension	−0.791 (−5.468 to 3.886)	0.734				
Self-reported diabetes	−0.594 (−9.593 to 8.404)	0.894				
Family history of glaucoma	−2.609 (−11.570 to 6.351)	0.559				
Cold extremities	−5.323 (−12.566 to 1.919)	0.145				
Migraine	−3.473 (−9.910 to 2.963)	0.282				

Values with statistical significance are in boldface.
*Only variables with p<0.1 in univariate analysis were included in the multivariate model.
BP, blood pressure; IOP, intraocular pressure; LCCI, lamina cribrosa curvature index; RNFL, retinal nerve fibre layer.

this hypothesis. The ONH with a larger LCCI may be under a greater mechanical strain, in which the laminar capillaries may be more prone to collapse, resulting in a smaller LCVD. This finding was observed in the treatment-naïve NTG eyes in this study, so it can be speculated that mechanical stress plays a role in eyes with low IOP both through the mechanical strain itself and via the impairment of perfusion.

On the other hand, the LCVD was not associated with the IOP, indicating that the LCVD might not be influenced simply by the IOP, but influenced by LC deformation. It can be speculated that the IOP itself does not fully represent the magnitude of

mechanical strain, while the LCCI does. The IOP did not differ between the healthy and NTG groups, whereas both the LCCI and LCVD did. This finding again supports the hypothesis that mechanical strain is better represented by the LCCI or LCVD than by the IOP. There could have been a positive association between IOP and LCVD if eyes with a higher IOP were included. However, this study only included treatment-naïve eyes with lower IOP, to exclude any potential influence of high IOP on either LCVD or LCCI.

There was no significant correlation between the LCCI and LCVD in the healthy group. The absence of a correlation may be

Table 3 Factors associated with the vessel density in the lamina cribrosa in healthy eyes

Variables	Univariate		Multivariate*	
	β (95% CI)	P value	β (95% CI)	P value
Age, *per 1 year older*	−0.060 (−0.205 to 0.084)	0.404		
Male gender	2.947 (−0.958 to 6.852)	0.135		
Central corneal thickness, *per 1 µm larger*	−0.015 (−0.076 to 0.046)	0.619		
Axial length, *per 1 mm larger*	0.644 (−0.948 to 2.236)	0.418		
Baseline IOP, *per 1 mm Hg higher*	−0.004 (−0.927 to 0.919)	0.993		
Global RNFL thickness, *per 1 µm larger*	0.258 (0.058 to 0.458)	**0.013**	0.233 (0.034 to 0.432)	**0.023**
Mean deviation, *per 1 dB larger*	−0.374 (−4.044 to 3.296)	0.838		
Mean LCCI, *per 1 unit larger*	−1.762 (−3.665 to 0.141)	0.069	−1.419 (−3.243 to 0.405)	0.124
Systolic BP, *per 1 mm Hg higher*	0.021 (−0.112 to 0.153)	0.756		
Diastolic BP, *per 1 mm Hg higher*	0.091 (−0.107 to 0.289)	0.358		
Mean arterial pressure, *per 1 mm Hg higher*	0.063 (−0.118 to 0.245)	0.484		
Mean ocular perfusion pressure, *per 1 mm Hg higher*	0.091 (−0.173 to 0.355)	0.490		
Self-reported hypertension	−1.528 (−5.807 to 2.751)	0.474		
Self-reported diabetes	−0.346 (−6.016 to 5.325)	0.902		
Family history of glaucoma	0.579 (−6.174 to 7.332)	0.863		
Cold extremities	1.431 (−3.877 to 6.738)	0.589		
Migraine	1.463 (−5.276 to 8.202)	0.663		

Values with statistical significance are in boldface.
*Only variables with p<0.1 in univariate analysis were included in the multivariate model.
BP, blood pressure; IOP, intraocular pressure; LCCI, lamina cribrosa curvature index; RNFL, retinal nerve fibre layer.
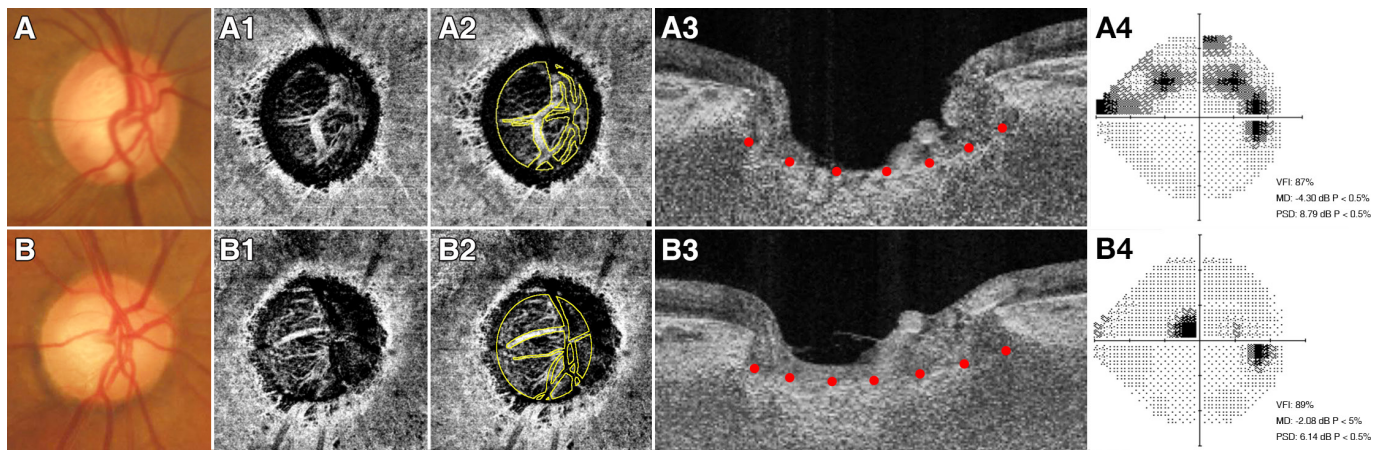
Figure 2 Treatment-naïve normal tension glaucomatous eyes with a larger (A) and a smaller (B) lamina cribrosa curvature index (LCCI), and with a smaller (A) and a larger (B) lamina cribrosa vessel density (LCVD). Colour disc images (A, B) and en face optical coherence tomography angiography (OCTA) images segmented in the layer of the lamina cribrosa (LC) (A1, B1). (A2, B2) Same images as (A1, B1) with the region of interest (ROI) indicated (area demarcated by the *yellow line*). (A3, B3) B-scan images after postprocessing by adaptive compensation. The LCVD is notably smaller in the eye with a larger LCCI (A3, *red glyphs*) than in the eye with a smaller LCCI (B3). (A4, B4) Greyscale plots of visual field test results.

attributable to an absence of, or a minimal degree of, mechanical strain in healthy eyes (ie, small LCCI), being insufficient to induce a decrease in the LCVD. On the other hand, it is also possible that microvessels in the LC maintain its perfusion despite the presence of a small LC deformation via autoregulation in healthy eyes. Autoregulation is an intrinsic ability of vascular beds to maintain a relatively constant blood flow over a large range of pressures.[22] The vascular bed of ONH in healthy eyes has been shown to maintain its autoregulatory capacity over a wide range of perfusion pressures.[23] In contrast, impaired autoregulation in the ONH has been reported in NTG.[24 25] The results of our study may be explained by the autoregulatory function being stronger in healthy eyes than in NTG eyes.[24 26]

We recently demonstrated that the reduction of the LCCI with surgical lowering of the IOP was associated with an increase in the LCVD in eyes with primary open-angle glaucoma.[13] This finding indicated that decreased mechanical stress would relieve the compressed RGC axons at the level of the LC and the compressed capillaries within the LC. It has been reported previously that the LC deformation decreases with surgical lowering of the IOP,[12 27] and such a decrease was associated with slower glaucoma progression.[27] IOP-lowering treatment might decrease mechanical stress and increase perfusion in the ONH, which could eventually enhance the treatment efficacy and halt or slow the progressive ONH damage. Reversal of the deformed LC has been reported also in NTG eyes after medical treatment,[28] prompting the need to further study to confirm whether IOP-lowering treatment increases the LCVD also in NTG eyes, and whether it is associated with disease prognosis.

Together with the LCCI, the RNFL thickness was significantly associated with the LCVD. Considering that the correlation was significant in both the NTG and healthy groups, the LCVD may also reflect the number of RGC axons with microvascular need. The overlap between the NTG and healthy groups was greater for the LCVD and the RNFL thickness than for the LCCI (figure 1). While the LCCI is a strong indicator of mechanical stress, the LCVD seems to reflect the perfusion status of viable axons along with the mechanical stress, rather than mechanical stress alone, which would explain its large overlap range in both groups. On the other hand, visual field MD was positively associated with the LCVD in NTG group but not in healthy group. This might be due to relatively small range of visual field MD in healthy group to observe the relationship with LCVD.

We found that a longer axial length was significantly associated with a smaller LCVD in the NTG group but not in the healthy group. Ren *et al*[29] reported that the LC thickness decreased significantly with increasing axial length in glaucomatous eyes, while such a relationship was not observed in normal eyes. Therefore, a smaller LCVD in the NTG eyes with a longer axial length could have been attributable to the thinner LC in those eyes.

The present study has limitations. The vessel density measured using OCTA might not completely represent the anatomical vessel density. In addition, the OCTA modality used in the present study has limitations in the analysis of segmented layers, especially the deeper layers, since artefacts due to vascular shadowing or projection onto the underlying tissues are unavoidable.[30 31] To overcome this limitation, we manually excluded vascular shadowing or projection artefacts from the en face images, and used binarised images. This approach resulted in only 1.9% of the eyes being excluded from the study due to the difficulty of visualising the LCVD using OCTA. In addition, there have been attempts to visualise microvessels in the deep ONH, and recent studies were able to successfully visualise the LCVD using OCTA.[13 32] On the other hand, it is possible that NTG eyes have inherently lower LCVD than healthy eyes. However, the correlation between LCVD and LCCI indicates that LCVD is somehow likely to be influenced by LCCI.

In conclusion, OCTA revealed a significant negative correlation between the LCCI and LCVD in treatment-naïve NTG eyes. The finding suggests that mechanical strain in the LC could affect ONH perfusion in eyes with NTG. Further studies are needed to determine whether the LCVD represents the true ONH perfusion, and whether the decreased perfusion is associated with the disease prognosis.

REFERENCES

1. Quigley HA, Addicks EM, Green WR, *et al*. Optic nerve damage in human glaucoma. II. The site of injury and susceptibility to damage. *Arch Ophthalmol* 1981;99:635–49.
2. Bellezza AJ, Rintalan CJ, Thompson HW, *et al*. Deformation of the lamina cribrosa and anterior scleral canal wall in early experimental glaucoma. *Invest Ophthalmol Vis Sci* 2003;44:623–37.
3. Yang H, Downs JC, Bellezza A, *et al*. 3-D histomorphometry of the normal and early glaucomatous monkey optic nerve head: prelaminar neural tissues and cupping. *Invest Ophthalmol Vis Sci* 2007;48:5068–84.
4. Strouthidis NG, Fortune B, Yang H, *et al*. Longitudinal change detected by spectral domain optical coherence tomography in the optic nerve head and peripapillary retina in experimental glaucoma. *Invest Ophthalmol Vis Sci* 2011;52:1206–19.
5. Quigley H, Anderson DR. The dynamics and location of axonal transport blockade by acute intraocular pressure elevation in primate optic nerve. *Invest Ophthalmol* 1976;15:606–16.
6. Gaasterland D, Tanishima T, Kuwabara T. Axoplasmic flow during chronic experimental glaucoma. 1. Light and electron microscopic studies of the monkey optic nervehead during development of glaucomatous cupping. *Invest Ophthalmol Vis Sci* 1978;17:838–46.
7. Burgoyne CF, Downs JC, Bellezza AJ, *et al*. The optic nerve head as a biomechanical structure: a new paradigm for understanding the role of IOP-related stress and strain in the pathophysiology of glaucomatous optic nerve head damage. *Prog Retin Eye Res* 2005;24:39–73.
8. Lee SH, Kim T-W, Lee EJ, *et al*. Diagnostic power of lamina Cribrosa depth and curvature in glaucoma. *Invest Ophthalmol Vis Sci* 2017;58:755–62.
9. Lee EJ, Kim T-W, Kim H, *et al*. Comparison between lamina Cribrosa depth and curvature as a predictor of progressive retinal nerve fiber layer thinning in primary open-angle glaucoma. *Ophthalmol Glaucoma* 2018;1:44–51.
10. Kim J-A, Kim T-W, Weinreb RN, *et al*. Lamina Cribrosa morphology predicts progressive retinal nerve fiber layer loss in eyes with suspected glaucoma. *Sci Rep* 2018;8.
11. Ha A, Kim TJ, Girard MJA, *et al*. Baseline lamina Cribrosa curvature and subsequent visual field progression rate in primary open-angle glaucoma. *Ophthalmology* 2018;125:1898–906.
12. Lee SH, Yu D-A, Kim T-W, *et al*. Reduction of the lamina Cribrosa curvature after trabeculectomy in glaucoma. *Invest Ophthalmol Vis Sci* 2016;57:5006–14.
13. Kim J-A, Kim T-W, Lee EJ, *et al*. Microvascular changes in peripapillary and optic nerve head tissues after trabeculectomy in primary open-angle glaucoma. *Invest Ophthalmol Vis Sci* 2018;59:4614–21.
14. Girard MJA, Strouthidis NG, Ethier CR, *et al*. Shadow removal and contrast enhancement in optical coherence tomography images of the human optic nerve head. *Invest Ophthalmol Vis Sci* 2011;52:7738–48.
15. Mari JM, Strouthidis NG, Park SC, *et al*. Enhancement of lamina cribrosa visibility in optical coherence tomography images using adaptive compensation. *Invest Ophthalmol Vis Sci* 2013;54:2238–47.
16. Ghasemi Falavarjani K, Al-Sheikh M, Akil H, *et al*. Image artefacts in swept-source optical coherence tomography angiography. *Br J Ophthalmol* 2017;101:564–8.
17. Al-Sheikh M, Ghasemi Falavarjani K, Akil H, *et al*. Impact of image quality on OCT angiography based quantitative measurements. *Int J Retina Vitreous* 2017;3.
18. Schneider CA, Rasband WS, Eliceiri KW. NIH image to ImageJ: 25 years of image analysis. *Nat Methods* 2012;9:671–5.
19. Schwartz B, Rieser JC, Fishbein SL. Fluorescein angiographic defects of the optic disc in glaucoma. *Arch Ophthalmol* 1977;95:1961–74.
20. Michelson G, Langhans MJ, Groh MJ. Perfusion of the juxtapapillary retina and the neuroretinal rim area in primary open angle glaucoma. *J Glaucoma* 1996;5:91???98–8.
21. Piltz-seymour JR, Grunwald JE, Hariprasad SM, *et al*. Optic nerve blood flow is diminished in eyes of primary open-angle glaucoma suspects. *Am J Ophthalmol* 2001;132:63–9.
22. Prada D, Harris A, Guidoboni G, *et al*. Autoregulation and neurovascular coupling in the optic nerve head. *Surv Ophthalmol* 2016;61:164–86.
23. Riva CE, Cranstoun SD, Petrig BL. Effect of decreased ocular perfusion pressure on blood flow and the flicker-induced flow response in the cat optic nerve head. *Microvasc Res* 1996;52:258–69.
24. Galambos P, Vafiadis J, Vilchez SE, *et al*. Compromised autoregulatory control of ocular hemodynamics in glaucoma patients after postural change. *Ophthalmology* 2006;113:1832–6.
25. Wang L, Cioffi GA, Cull G, *et al*. Immunohistologic evidence for retinal glial cell changes in human glaucoma. *Invest Ophthalmol Vis Sci* 2002;43:1088–94.
26. Pillunat LE, Stodtmeister R, Wilmanns I. Pressure compliance of the optic nerve head in low tension glaucoma. *Br J Ophthalmol* 1987;71:181–7.
27. Lee EJ, Kim T-W. Lamina Cribrosa reversal after trabeculectomy and the rate of progressive retinal nerve fiber layer thinning. *Ophthalmology* 2015;122:2234–42.
28. , , Weinreb RN, *et al*. Reversal of lamina cribrosa displacement after intraocular pressure reduction in open-angle glaucoma. *Ophthalmology* 2013;120:553–9.
29. Ren R, Wang N, Li B, *et al*. Lamina cribrosa and peripapillary sclera histomorphometry in normal and advanced glaucomatous Chinese eyes with various axial length. *Invest Ophthalmol Vis Sci* 2009;50:2175–84.
30. Spaide RF, Fujimoto JG, Waheed NK. Image artifacts in optical coherence tomography angiography. *Retina* 2015;35:2163–80.
31. Akagi T, Iida Y, Nakanishi H, *et al*. Microvascular density in glaucomatous eyes with hemifield visual field defects: an optical coherence tomography angiography study. *Am J Ophthalmol* 2016;168:237–49.
32. Numa S, Akagi T, Uji A, *et al*. Visualization of the lamina Cribrosa microvasculature in normal and glaucomatous eyes: a Swept-source optical coherence tomography angiography study. *J Glaucoma* 2018;27:1032–5.